BOOK OF PROCEEDINGS
(Available at: http://acsnigeria.org/publications/proceedings)

Green Synthesis of Silver Sulfide Nanoparticles from *Musa paradisiaca* Extract for Corrosion Inhibition of Mild Steel in 0.5 M Sulphuric Acid

Sylvester O. Adejo [1†], Victor O. Egbeneje [1†*], Joseph A. Gbertyo [1†], Samuel E. Okhale [2‡], Isaac O. Ogbogo [3†] and Simeon O. Enyi[4‡]

[1]Department of Chemistry, Benue State University, P. M. B 102119, Makurdi, km 1, Gboko Road, Benue State, Nigeria.
[2]Department of Medicinal Plant Research and Traditional Medicine, National Institute for Pharmaceutical Research and Development (NIPRD), Abuja, Nigeria
[3]Department of Chemistry, Sam Houston State University, USA
[4]Department of Epidemiology and Evidence-Based Medicine, Sechenov First Moscow State Medical University Russia

***Corresponding Author's E-mail:** egbenejevictor2018@gmail.com **Phone:** +2348085576834

ABSTRACT

Corrosion attack affects the functionality of metallic materials in industrial installations. The material is usually protected from these effects by the use of inhibitors. As an alternative to synthetic chemical/inorganic inhibitors, researchers are exploring environmentally friendly solutions, such as natural products like essential oils, for protecting these metals against corrosion. Nanomaterials are increasingly being applied in various fields due to their effective properties. This study explores the green synthesis of silver sulfide nanoparticles using an aqueous extract of *Musa paradisiaca* peels as reducing, capping, and stabilizing agents for inhibition of corrosion of mild in sulphuric acid medium. The nanoparticles were characterized using Fourier Transform Infrared Spectroscopy (FTIR) and UV-Vis Spectroscopy. The UV-Vis spectrum revealed a strong emission peak at 400 nm, indicating the presence of Ag_2S nanoparticles. FTIR spectra showed functional groups such as alcohol/phenol –OH, carboxylic acid –OH, and N-H of amides, with a notable C=C stretch at 1620 cm^{-1}. The synthesized nanoparticles effectively reduced corrosion when applied to mild steel. The study found that higher nanoparticle concentrations and higher temperatures enhanced their protective effects, suggesting a strong chemical interaction between nanoparticles and the metal surface. This protective mechanism aligns with fundamental principles of chemical adsorption. Adsorption isotherms, including Tempkin Langmuir, Freundlich, and Adejo Ekwenchi, confirmed the chemisorptive nature of the process. Overall, this research highlights a promising pathway for developing eco-friendly corrosion inhibitors using natural resources and advanced nanotechnology.

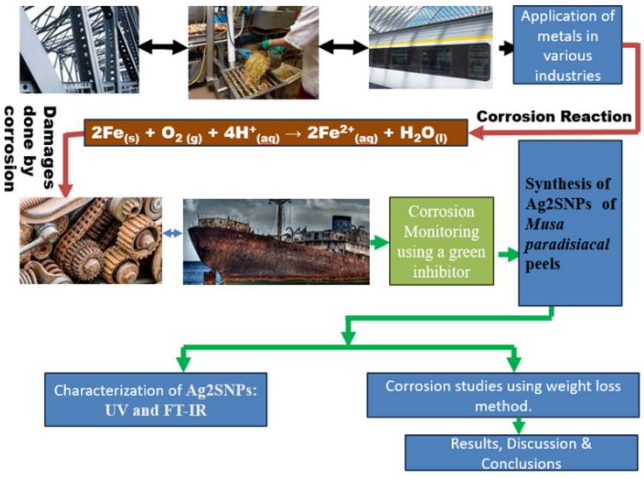

KEYWORDS: Synthesis, Corrosion, Nanoparticles, *Musa paradisiaca*, Isotherms.

1. INTRODUCTION

Finding corrosion inhibitors that are environmentally safe and readily available has been a growing trend among scientists and engineers. Among the known nanoparticles, silver nanoparticles (Ag-NPs) are most commonly and widely used. [1-11] due to their versatility of applications. Studies have shown that sulfidation of Ag-NPs effectively reduces its toxicity. However, the ease with which Ag_2S-NPs may transform in some environments leading to the initial rapid release of dissolved Ag(I) and subsequent formation of Ag^0-NPs suggests that Ag_2S-NP is highly safe [12]. Several research has been carried out to evaluate the medicinal and nutritional potent, traditional anti-diabetic agent, and many other

pharmacological activities of *Musa paradisiaca*. [13] The extract of this plant converted to silver sulfide nanoparticles, which contain many environmentally friendly compounds, may be utilized as eco-friendly corrosion inhibitors. This present study investigated the inhibitive potential of *Musa paradisiaca* peels silver sulfide nanoparticles through thermodynamic, kinetic, and adsorptive parameter studies.

2. MATERIALS AND METHODS

2.1. Plant extraction and green synthesis of silver sulfide (Ag_2SNP) using *Musa paradisiacal* peels

Musa paradisiaca peels, authenticated at the Department of Biological Sciences, Benue State University, Makurdi, were dried to a constant weight after 7 days. After crushing and pounding into powder, 20 g was weighed into an 800 mL conical flask, and 200 mL of distilled water was added. The mixture was boiled for 10 minutes using a heating mantle/hot plate. The solution, thereafter, was cooled and filtered into a 250mL conical flask to obtain an aqueous extract.

Green synthesis of silver sulfide nanoparticles was done by reacting silver nitrate solution with *Musa paradisiaca* peels aqueous extract and sodium sulfide at 27 °C using 1g of silver nitrate dissolved in 100 ml of *Musa paradisiacal* peels aqueous extract under magnetic stirring for 10 minutes. A solution of sodium sulfide containing 1 g was prepared in 100 ml of distilled water and gently swirled for homogeneity. The sodium sulfide solution was then added dropwise to the mixture of $AgNO_3$ solution and *Musa paradisiaca* peel extract under continuous magnetic stirring until the color of the solution changed to a suspended gray-black color, an indication of the formation of silver sulfide nanoparticles. [14] Thereafter, the mixture was centrifuged at 8000 rpm for 4 hours, the supernatant removed, and the precipitate collected and rinsed with 5 mL of distilled water. The obtained nanoparticles were transferred to a sample bottle and kept for further work.

2.2. Preparation of the coupon

Coupons of dimension 2 cm x 1.9 cm x 0.1 cm were prepared from mild steel rods purchased from the open market in Makurdi, and a tiny hole was drilled at the edge of each for suspension. After polishing to mirror finish the coupons using sandpaper, the coupons were degreased in acetone, and preserved in a desiccator. Subsequently, the initial weights (W_i) of the coupons were then made ready for corrosion studies. [15-19]

2.3. Corrosion studies

A 0.5 M solution of H_2SO_4 was prepared which served as the corrodent. Thereafter, the weighed coupons were placed in various concentrations of silver nanoparticles (0, 1, 2, 3, 4, 5) gdm^{-3} in 50 ml of the 0.5 M H_2SO_4. The corrodent with/without the inhibitor and coupons were placed in the thermostatic water bath set at 301 K for 6 hours. After the time interval, the coupons were removed, quenched in saturated ammonium acetate solution, washed in distilled water, and dried in acetone, kept in a desiccator, and then the final weight (W_f) was taken, thereafter. The procedure was repeated at 305 K, 309 K, and 313 K.

2.4. Weight loss measurement

The weight loss, inhibition efficiency (%IE), and corrosion rate (CR) was calculated using equations (1), (2) and (3), respectively as reported by different scholars. [6-10]

$$WL = W_I - W_F \quad (1)$$

$$\%IE = \left[1 - \frac{W_1}{W_2}\right] \times 100 \quad (2)$$

$$CR\ (mgcm^{-2}h^{-1}) = \frac{WL}{At} \quad (3)$$

where WL is the weight loss of the coupon, W_I is the weight before insertion, and W_F is the weight after retrieval, w_1 *and* w_2 are the weight losses (in grams) of mild steel coupon in the presence and absence of the inhibitor in the acid solution, WL is the weight loss in milligrams (mg), A the coupon surface area in cm^2, and t is the immersion time in hours. Equations (4) to (7) are used for the evaluation of activation energy, the heat of adsorption, enthalpy of activation and entropy, and Gibb's free energy, respectively.

$$logCR = logA - \frac{E_a}{2.303RT} \quad (4)$$

$$log\left(\frac{\theta}{1-\theta}\right) = LogA + LogK - \frac{Q_{ads}}{2.303R}\left(\frac{1}{T}\right) \quad (5)$$

$$ln\left(\frac{CR}{T}\right) = \ln\left(\frac{R}{Nh}\right) + \frac{\Delta S^*}{R} - \frac{\Delta H^*}{RT} \quad (6)$$

$$\Delta G_{ads} = -RT\ln(55.5\ K) \quad (7)$$

where K= $\frac{\theta}{(1-\theta)c}$, C is the concentration of the extract and 55.5 is the concentration of water expressed in moles. [24]

Langmuir, Freundlich, Temkin, and Adejo-Ekwenchi, adsorption isotherms (Equation 9-12 were used to model the adsorption process.

Langmuir $\frac{C}{\theta} = \frac{1}{K} + C$ (9)

Temkin $\frac{-2\alpha\theta}{2.303} = logK + logC$ (10)

Freundlich $log\theta = logK + nlogC$ (11)

Adejo-Ekwenchi $log\frac{1}{(1-\theta)} = logK_{AE} + blogC$ (12)

where K is the equilibrium constant, C is the concentration of the inhibitor, and n is a constant that tells the intensity of the adsorption process and has a typical value of 0.6 [24].

3. RESULTS AND DISCUSSION

3.1. Results

3.1.1 Characterization of Sample

In this study ultraviolet (UV) and Fourier-transform infrared (FTIR) spectroscopy were used in the context of our research objectives. UV spectroscopy, widely employed for identifying and quantifying chemical compounds, operates by measuring the absorption of UV light by molecules, which provides insights into electronic transitions, conjugation, and the structural features of organic and inorganic substances. FTIR spectroscopy, on the other hand, is a powerful analytical tool for characterizing molecular vibrations, yielding detailed information about functional groups and molecular interactions. Together, these spectroscopic techniques allow for a comprehensive analysis of the compounds under study, enhancing our understanding of their photochemical and structural properties. Below are the specific results obtained from UV and FTIR spectra as well as corrosion studies. The discussions highlight the significance of the UV and FTIR spectra in the characterization process and the effect of silver sulfide (Ag_2SNP) using *Musa paradisiacal* peels in mitigating corrosion of mild still

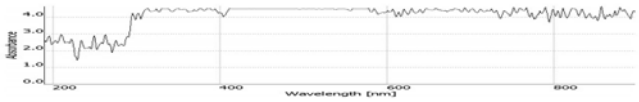

Fig 1: UV-vis spectral AgSNPs from *Musa paradisiaca* peels extract

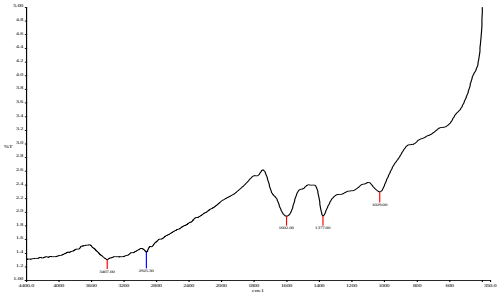

Fig 2: FT-IR spectral of AgSNPs from *Musa paradisiaca peels* extract

3.1.2. Corrosion studies

(a). Effect of Inhibitor Concentration

The values of weight losses (WL), inhibition efficiency (%IE), Surface coverage, and corrosion rate for the inhibition of mild steel corrosion by silver sulfide nanoparticles of *Musa paradisiacal peels* extract 0.5 M sulphuric acid at various concentrations and temperatures are presented in Table1 and 2, respectively.

Table 1: Weight Loss and Inhibition Efficiency for silver sulfide nanoparticle of *Musa paradisiacal peels* extract

Concentration	WL (g)				%IE			
(g/dm^3)	301K	305K	309K	313K	301K	305K	309K	313K
Blank	0.0548	0.0836	0.1159	0.1678				
0.1	0.0393	0.0564	0.0735	0.0989	28.2847	32.5359	36.5833	41.0608
0.2	0.0370	0.0489	0.0628	0.0878	32.4818	41.5072	45.8154	47.6758
0.3	0.0340	0.0374	0.0456	0.0629	37.9562	55.2632	60.6557	62.5149
0.4	0.0292	0.0309	0.0407	0.0531	46.7153	63.0383	64.8835	68.3552
0.5	0.0230	0.0249	0.0340	0.0389	58.0292	70.2153	70.6644	76.8176

Table 2: Corrosion rate for silver sulfide nanoparticle of *Musa paradisiacal* peels

Concentration	CR			
(g/dm^3)	301K	305K	309K	313K
Blank	12.6852	19.3519	26.8287	38.8426
0.1	9.0972	13.0556	17.0139	22.8935
0.2	8.5648	11.3194	14.5370	20.3241
0.3	7.8704	8.6574	10.5556	15.9491
0.4	6.7593	7.1528	9.4213	12.2917
0.5	5.3241	5.7639	7.8704	9.0046

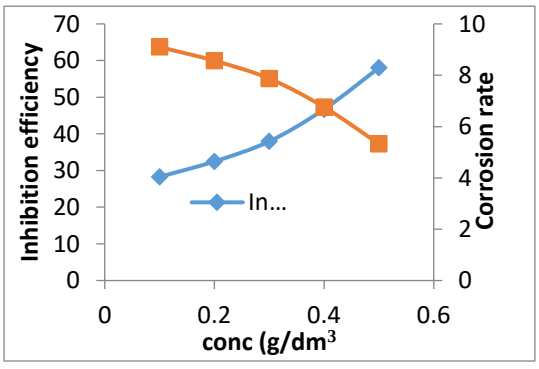

Figure 1: Variation CR and %IE at 301K.

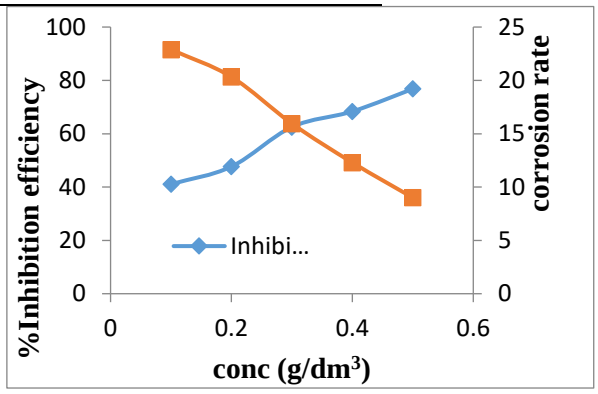

Figure 2: CR and %IE at 313K.

(b). Effect of temperature

The effect of temperature on the corrosion behavior of steel in 0.5 M H_2SO_4 containing AgSNPs from *Musa paradisiacal* peels 0.1 -0.5 g/dm^3 is studied in the temperature range of 301-313 K using weight loss measurements for 6 hrs. The data of corrosion rates (W) and corresponding inhibition efficiency (%IE) collected were presented in Tables 1 and 2 above. Figures 3 and 4 show the effect of temperature on the corrosion behavior of mild steel in 0.5 M H_2SO_4 containing AgSNPs from *Musa paradisiacal* peels at o.1 and 0.5 g/dm^3 only.

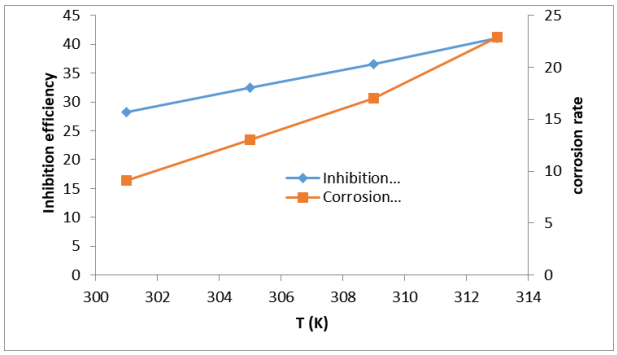

Figure 3: Variation of CR and %IE in 0.1g/dm^3 at different temperatures

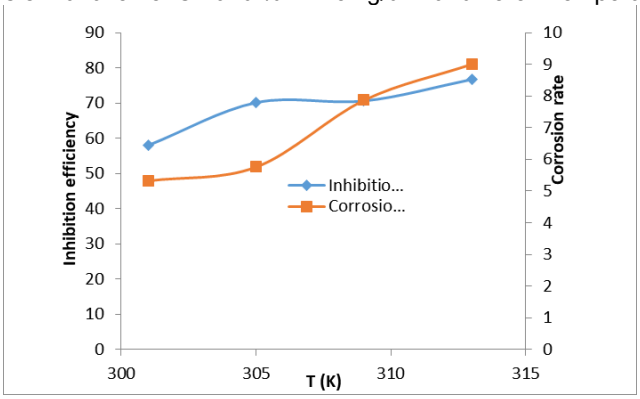

Figure 4: Variation of CR) and %IE in 0.5g/dm^3 at different temperatures

Table 3: Values of activation energy and thermodynamic parameters for silver sulfide nanoparticle of *Musa paradisiacal* peels as inhibitor for mild steel corrosion.

Conc. (g/dm^3	E_a (kJ/mol)	$+\Delta H^*$ ads (kJ/mol)	$+\Delta S^*$ ads (kJ/mol)	$+Q_{ads}$ (kJ/mol)	-ΔG ads (kJ/mol) 301 K	305 K	309 K	313 K
Blank	70.94	68.42	386.45	-				
0.1	58.37	55.85	341.97	80.09	13.49	14.18	14.82	15.51
0.2	54.96	52.44	329.83	39.67	12.25	13.40	14.02	14.40
0.3	45.42	42.90	296.91	51.93	11.84	13.78	14.52	14.53
0.4	40.25	37.73	278.53	52.85	12.02	13.86	14.25	14.84
0.5	36.32	33.81	263.84	50.84	12.60	14.12	14.36	15.38

(c). Effects of adsorption parameters

In the present study, the following adsorption isotherms were used to model the adsorption process of the inhibitor: Langmuir, Freundlich, Temkin, and Adejo Ekwenchi, isotherms.

Table 4: The Adsorption Parameters of Adsorption Isotherms

Langmuir	R^2	Kad	Constant	$-\Delta G_{ads}$
301K	0.850	0.7962		9.4823
305K	0.964	1.0395		10.2847
309K	0.982	0.9542		10.1996
313K	0.959	1.0040		10.4640
Freundlich			ɲ	

301K	0.896	0.6998	0.426	9.1594
305K	0.985	0.9817	0.492	10.1396
309K	0.979	0.9616	0.425	10.2194
313K	0.960	0.9727	0.395	10.3816
Temkin			α	
301K	0.830	4.3251	-0.4514	13.7183
305K	0.962	6.9984	-0.6318	15.1211
309K	0.969	7.0958	-0.5792	15.3550
313K	0.928	7.6384	-0.5873	15.7455
Adejo Ekwenchi			b	
301K	0.777	2.5586	0.297	12.4044
305K	0.916	4.2858	0.495	13.8773
309K	0.948	4.4978	0.483	14.1835
313K	0.863	5.3703	0.553	14.8286

3.2. Discussion

3.2.1. Synthesis and characterization

A simple method using plant extract reduction has been developed for synthesizing silver nanoparticles, which could also be used for the synthesis of several metallic nanoparticles involving other metals with good size and shape morphology. [25] The results related to the metallic silver sulfide nanoparticles indicated the reduction of silver ions by *Musa paradisiaca* peels. Therefore, it can be concluded that the non-active or stationary cells of *Musa paradisiaca* peels can reduce silver ions in their periplasmic space. Initially, the synthesis of silver sulfide nanoparticles was confirmed by observing the color change of the reaction mixture [26, 27]. The appearance of a suspended gray-black color at room temperature suggested the formation of silver sulfide nanoparticles. The confirmation of formation and stability of the silver sulfide nanoparticles in the colloidal solution was monitored by using UV-Vis spectral analysis and FTIR. Ultraviolet-visible (UV-vis) spectra from 200 to 700 nm were measured using a Shimadzu UV-vis spectrophotometer (UV-3600, Japan). Silver sulfide nanoparticles usually exhibit strong absorbance in the range of 200-600 nm revealing good photo absorption properties. In Fig 1 above the spectrum revealed that the synthesized silver sulfide nanoparticles exhibit a powerful emission peak at 400 nm characteristic of Ag_2SNPs nanoparticle, due to its surface Plasmon resonance absorption band. [26, 27]

FTIR measurements were carried out to identify the possible biomolecules responsible for the reduction of the silver ions, and capping of the bio-reduced silver sulfide nanoparticles synthesized by *Musa paradisiaca* peels extract filtrate. Representative spectra of nanoparticles obtained from FTIR measurements manifested absorption peaks located at about 3407.00, 2925.30, 1602.00, 1377.00, and 1029.00 cm^{-1}. The FTIR spectra revealed the presence of different functional groups like the alcohol/phenol –OH stretching vibration, carboxylic acid –OH stretch, and N-H stretching of amides. The strong peak at 1620 cm^{-1} is characterized by alkene. It can be deduced that the flavonoids and terpenoids, which are abundant in *Musa paradisiaca*, show characteristic absorption peaks that appear to be responsible for the accelerated reduction and capping process, which give rise to the well-known signatures in the infrared region of the electromagnetic spectrum (Fig. 2). [28]

3.2.2. Effect of concentration and temperature

The effect of concentration and temperature on the corrosion of mild steel in 0.5 M sulphuric acid using silver sulfide nanoparticles synthesized from *Musa paradisiaca* peel extract as an inhibitor was investigated and the results are presented in Tables 1 and 2, respectively. Table 1 shows the values of weight loss and percentage inhibition efficiency of the inhibitor at various concentrations in an acid solution. The reduction in weight loss on the introduction of the nanoparticles into the corrodent is an indication that the silver sulfide nanoparticles of *Musa paradisiaca* have an inhibitive effect. [29] This percentage inhibition efficiency was observed to increase with the increase in the concentration of synthesized silver sulfide nanoparticles of *Musa paradisiaca*l peel extract with an increase in

temperature (Fig. 1 and 2 at 301K and 313K). The highest inhibition efficiency of 76.8176% was obtained at 0.5 g dm^{-3} at 313 K and the least is 28.28 % at 301K for 0.1dm^{-3} concentrations. There is a significant difference between the values of % I. E with temperature rise which is suggestive of chemical adsorption mechanism (Fig. 3 and 4 at 0.1 g/dm^3 and 0.5 g/dm^3, respectively). [29]

Table 2 shows the surface coverage and corrosion rate for the inhibition of mild steel corrosion by silver sulfide nanoparticles of *Musa paradisiaca*l peels at various concentrations and temperatures. The corrosion rate which was observed to be high in the blank, significantly reduced as seen in the corrosion rate upon introduction of the inhibitor into the corroding medium. This indicates that the synthesized silver sulfide nanoparticles of *Musa paradisiaca*l peel extracts can be effectively used to mitigate the rate of mild steel in the acid medium. It was observed that the corrosion rate of the mild steel decreased with an increase in concentration and increased with an increment in temperature (Fig. 1, 2, 3, and 4]. This behavior explains the fact that the extent of adsorption and the coverage of inhibitor on mild steel surface increases with inhibitor concentration. [30]

This outcome demonstrates the capacity of Musa paradisiaca-derived nanoparticles to reduce the corrosion rate in an acidic environment. Similarly, studies by Zhang et al. (2021) on green inhibitors derived from plant extracts have shown that these natural inhibitors effectively reduce corrosion rates by forming a protective film on the steel surface, especially when used in higher concentrations. [31]

Furthermore, the corrosion rate inversely correlates with inhibitor concentration but directly correlates with temperature increases, as observed in this study's results (Fig. 1, 2, 3, and 4). This trend is consistent with findings in similar research, where higher temperatures weaken the adsorption bond between the inhibitor molecules and the metal surface, reducing its effectiveness at elevated temperatures. [32] The observed decline in corrosion rates with higher inhibitor concentrations aligns with findings in related research on plant-based nanoparticle inhibitors, where the extent of adsorption and surface coverage on mild steel increased with inhibitor concentration, leading to more efficient protection. [33]

3.2.3. Activation energy and thermodynamic parameters for the inhibition process

The activation and thermodynamic parameters for the inhibition process for the nanoparticles are presented in Table 3. Computed values of activation energy values are all positive and significantly lower than those of the blank as shown in Table 3. Lower values of $E_{a.}$ in the presence of an inhibitor than in the absence of it suggest that the process is chemisorption while the reverse (higher) is an indication of physisorption. [24, 34] The enthalpy of activation (ΔH^*_{ads})which is a measure of the height of the energy barrier that has to be overcome by the reactant to attain a transition state. Computed values of enthalpy of activation are all positive and lower than that of the blank as shown in Table 3 indicating that the efficiency of inhibition increased with an increase in temperature. [35, 36] The dissolution process was also endothermic as the values were all positive. The average difference of $E_{a.}$ – ΔH* was found to be 2.52 kJolmol^{-1} [approximately equal to 2.55 kJmol^{-1} which is the value of RT (R is the universal gas constant and T is the average of the temperature at which the studies were conducted)]. This implies that the corrosion process of the metal in a medium is an unimolecular reaction.[37] The entropy of activation(ΔS^*_{ads}) values for the inhibitor are given in Table 3. The shift towards the positive value of entropies (S*) implies that the activated Complex in the rate-determining step represents dissociation rather than association, meaning that disorderliness increases on going from reactants to the activated complex.[38, 39]

The heat of adsorption (Q_{ads}) for all inhibitors were all positive indicating that the processes were endothermic. This means absorption of energy from the surroundings was required for the reaction to be sustained. [40]

The values of Gibbs free energy (ΔG_{ads})for adsorption in aqueous solution are usually around -20 kJ mol^{-1} or lower (more positive) which indicate that the adsorption is due to electrostatic interaction between the inhibitor and metal (physisorption). While those around or higher (more negative) than -40 kJ mol^{-1} involve charge sharing or transfer of electrons between the molecules and metal (chemisorption). [41, 42] The negative ΔGads values in Table 3 indicate that adsorption is spontaneous,

meaning it occurs naturally without external energy input. As the temperature increases, these values become less negative, suggesting that while the process remains spontaneous, its driving force diminishes with rising temperature. The stability of the adsorption values being below or slightly above -20 kJ mol^{-1} further signifies that the adsorption mechanism is likely physical adsorption (physisorption), which involves weaker interactions compared to chemical The negative (ΔG_{ads})values in Table 3 suggest that the adsorption process is spontaneous, aligning with similar research findings (Hassan & Mohamed, 2018)., [43 44] where an increase in temperature resulted in less negative (ΔG_{ads}) values, indicating a decrease in the spontaneity or driving force for adsorption.

As observed in prior studies, the lower magnitude of (ΔG_{ads}) , often below -20 kJ mol^{-1}, supports the conclusion that the adsorption mechanism is physisorption. This process is typically reversible and relies on weaker forces, unlike chemisorption, which is usually stronger and less reversible (Chen et al., 2021). [45] This trend aligns with the work of Hassan and Mohamed (2018) [44], who noted a similar reduction in spontaneity with temperature, suggesting that increased thermal energy diminishes the attraction between the inhibitor and metal surface.

3.2.4. Adsorption isotherm for the inhibition process

The mechanism and action of inhibition have been attributed to the adsorption process of the adsorbate (inhibitor) onto the surface of the metal (adsorbent); hence adsorption isotherm models have been extensively used in its confirmation. In the present study, the data obtained from weight loss method were fitted into the various two-parameter isotherms. Going by the coefficient of determination (R^2) the adsorption process can be said to fit into the Langmuir, Freundlich, Temkin, and Adejo Ekwenchi isotherms.

(a) Langmuir Isotherm: Langmuir isotherm adsorption is usually an indication of monolayer coverage of inhibitor on the surface of mild steel. The slopes and intercepts are given in Table 4, along with the coefficient of determination (R^2) for nanoparticles of silver sulfide synthesized from *Musa paradisiaca*l peel extracts. An ideal Langmuir isotherm plot should have a good R^2 value (unity) and intercept of zero (Fig. 5a) with a positive adsorption equilibrium constant K [46]**.** In reference to the values of regression coefficient R^2 as shown in Table 4, the adsorption equilibrium constant K values are positive and intercept close to zero indicative of the suitability of the Langmuir isotherm to the adsorption behavior of inhibitors. Langmuir isotherm applies to both physisorption and chemisorption. Hence Langmuir isotherm can be used to model the adsorption of this study.

(b) Temkin Isotherm: The Isotherm constant and coefficient of determination of (R^2) are presented in Table 4 and Fig. 5b. The constant α which is related to the heat of adsorption, equally increases with an increase in temperature, which is a characteristic of chemisorption. Examination of the data shows that the Temkin isotherm applies to the inhibitor adsorption on mild steel and the adherence of this adsorption layer. The negative values of "α" are indications of repulsive interaction in the absorbed layer, the increase in the value of ΔG_{ads} with temperature rise is a feature of chemical adsorption. [40]

(c) Freundlich Isotherm: The Freundlich constant has to do with the adsorption intensity and the heterogeneity of the material, and its good value should be close to 0.6. [47] The values of the parameter n_f obtained were not close to 0.6 The fact that the obtained average value of n (0.4345) is not close to 0.6 implies that this adsorption process cannot be modeled by this isotherm. [48, 49] despite having a good value of regression coefficient (R^2)

(d) Adejo Ekwenchi Isotherm: Values of regression coefficient (R^2) of Adejo-Ekwenchi Isotherm can be seen in Table 4 and Fig. 5d. Adejo-Ekwenchi Isotherm as it seems to be obeyed by nearly any adsorption process, is centered on the fact that for any adsorption process, the available surface of a given quantity of the adsorbent decreases with increase in the concentration of the adsorbate. Hence the difference between the total available surface on the adsorbent and the fractional surface coverage decreases with an increase in the adsorbate concentration, that is, the more the surface coverage the less the available surface. Therefore, there is an inverse relationship between the available surface and the concentration of the adsorbate. [35] A decrease in the b value with temperature rise signifies physisorption, while an

increase or fairly constant value indicates chemisorption. From Table 4, it is obvious that the absorption of the inhibitors onto the metal surface is chemisorption, as b increases with temperature or is fairly constant.

4. CONCLUSION

The results related to the metallic silver sulfide nanoparticles indicate the reduction of silver ions by *Musa paradisiaca* peels. Therefore, it can be concluded that the resting cells of *Musa paradisiaca* peels can reduce silver ions in their periplasmic space. The confirmation of formation and stability of the silver sulfide nanoparticles in the colloidal solution was monitored by using UV-Vis spectral analysis and FTIR. From the above results, it has been shown that silver sulfide nanoparticles of *Musa paradisiaca* peels extract are a good inhibitor that can be used when developed to mitigate the rate of corrosion since it is environmentally benign as this will greatly enhance global sustainability.

ACKNOWLEDGEMENTS

The authors are profusely appreciative of the Royal Society of Chemistry for the sponsorship provided to attend the 1st ACS Africa Regional Conference on Green and Sustainable Chemistry, Lagos, Nigeria, 2024. We are grateful to the Management of Benue State University, Makurdi for providing the enabling environment for the successful completion of this research. Our gratitude also goes to the staff of the Departments of Biological Sciences and Chemistry Laboratories of our great institution for assistance.

CONFLICT OF INTEREST: The authors declare no conflict of interest.

REFERENCES

(1) Ikeuba, A. I.; Ita, B. I.; Etiuma, R. A.; Bassey, V. M.; Ugi, B. U.; Kporokpo, E. B. Green Corrosion Inhibitors for Mild Steel in H_2SO_4 Solution: Flavonoids of Gongronema latifolium. Chem. Process Eng. Res. **2015**, 34, 2224–7467.
(2) Ali, A.; Hummza, R.; Balakit, A.; Al-Amiery, A.; Yousif, E. Synthesis of New 3-[(4-Bromo-5-Methylthiophen-2-yl) Methylene Amino]-2-Isopropyl Quinazolin-4(3H)-One and Its Corrosion Inhibition on Zinc by 2M Hydrochloric Acid. Yanbu J. Eng. Sci. **2016**, 13, 11–19.
(3) El Bribri, A.; Tabyaoui, M.; Tabyaoui, B.; El Attari, H.; Bentiss, F. The Use of Euphorbia Falcata Extract as Eco-Friendly Corrosion Inhibitor of Carbon Steel in Hydrochloric Acid Solution. Mater. Chem. Phys. **2013**, 141, 240–247.
(4) Andreani, S.; Znini, M.; Paolini, J.; Majidi, L.; Hammouti, B.; Costa, J.; Muselli, A. Study of Corrosion Inhibition for Mild Steel in Hydrochloric Acid Solution by Limbarda Crithmoides (L.) Essential Oil of Corsica. J. Mater. Environ. Sci. **2016**, 7 (1), 187–195.
(5) Ahmed, A. A.; Al-Mashhadani, M. H.; Hussain, Z.; Mohammed, S. A.; Yusop, R. M.; Yousif, E. Inhibition of Corrosion: Mechanisms and Classifications—An Overview. Al-Qadisiyah J. Pure Sci. **2020**, 25 (2), 1–9.
(6) El-Haddad, N. Chitosan as a Green Inhibitor for Copper Corrosion in Acidic Medium. Int. J. Biol. Macromol. **2013**, 55, 142–149.
(7) Andreani, S.; Znini, M.; Paolini, J.; Majidi, L.; Hammouti, B.; Costa, J.; Muselli, A. Study of Corrosion Inhibition for Mild Steel in Hydrochloric Acid Solution by Limbarda Crithmoides (L.) Essential Oil of Corsica. J. Mater. Environ. Sci. **2016**, 7 (1), 187–195.
(8) Manssouri, M.; Znini, M.; Ansari, A.; Bouyanzer, A.; Faska, Z.; Majidi, L. Odorized and deodorized aqueous extracts of Ammodaucus leucotrichus fruits as green inhibitor for C38 steel in hydrochloric acid solution. Der Pharma Chem. **2014**, 6 (6), 331–345.
(9) Manssouri, M.; El Ouadi, Y.; Znini, M.; Costa, J.; Bouyanzer, A.; Desjobert, J.-M.; Majidi, L. Adsorption properties and inhibition of mild steel corrosion in HCl solution by the essential oil

from fruit of Moroccan Ammodaucus leucotrichus. Mater. Environ. Sci. **2015**, 6 (3), 631–646. ISSN: 2028-2508.

(10) Dhaka, A.; Mali, S. C.; Sharma, S.; Trivedi, R. A Review on Biological Synthesis of Silver Nanoparticles and Their Potential Applications. Results Chem. **2023**, 6, 101108. https://doi.org/10.1016/j.rechem.2023.101108.

(11) Sun, Z.; Hafez, M. E.; Ma, W.; Long, Y.-T. Recent Advances in Nanocollision Electrochemistry. *Science China Chemistry* **2019**, *62* (12), 1588–1600. https://doi.org/10.1007/s11426-019-9529-x.

(12) He, D.; Garg, S.; Wang, Z.; Li, L.; Rong, H.; Ma, X.; Li, G.; An, T.; Waite, T. D. Silver Sulfide Nanoparticles in Aqueous Environments: Formation, Transformation and Toxicity. Environ. Sci. Nano **2019**, 6, DOI: [if available].

(13) Imam, M. Z.; Akter, S. Musa Paradisiaca L. and Musa Sapientum L.: A Phytochemical and Pharmacological Review. J. Appl. Pharm. Sci. **2011**, 1 (5), 14–20.

(14) Awwad, M. A.; S., N. M.; A., M. M.; A., F. M. Green Synthesis, Characterization of Silver Sulfide Nanoparticles and Antibacterial Activity Evaluation. J. Chem. Int. Sci. Organ. **2020**, 6 (1), 42–48.

(15) Adejo, S. O. Proposing a New Empirical Adsorption Isotherm Known as Adejo-Ekwenchi Isotherm. IOSR J. Appl. Chem. **2014**, 6 (5), 66–71. DOI: 10.5736-0656671.

(16) Adejo, S. O.; Gbertyo, J. A.; Ahile, J. U. Inhibitive Properties and Adsorption Consideration of Ethanol Extract of Manihot Esculentum Leaves for Corrosion Inhibition of Aluminium in 2 M H_2SO_4. Int. J. Mod. Chem. **2013**, 4 (3), 137–146.

(17) Adejo, S. O.; Ekwenchi, M. M.; Odiniya, E. O.; Acholo, J. P.; Banke, S. P. Ethanol Extract of Leaves of Portulaca Oleracea as Green Inhibitor for Corrosion of Mild Steel in H_2SO_4 Medium. Proc. Int. Conf. Res. Dev., Accra, Ghana, **2010**, 113–118.

(18) Adejo, S. O.; Ekwenchi, M. M.; Gbertyo, J. A.; Menenge, T.; Ogbodo, J. O. Determination of Adsorption Isotherm Model Best Fit for Methanol Leaf Extract of Securinega Virosa as Corrosion Inhibitor for Corrosion of Mild Steel in HCl. J. Adv. Chem. **2014**, 10 (5).

(19) Adejo, S. O.; Ekwenchi, M. M.; Banke, S. P. Ethanol Extract of Leaves of Manihot Esculentum as Eco-Friendly Inhibitor for Corrosion of Mild Steel in H_2SO_4 Medium. Proc. 33rd Annu. Int. Conf. Chem. Soc. Niger., Osun, **2010**, 240–244.

(20) Adejo, S. O.; Ekwenchi, M. M.; Gbertyo, J. A.; Menenge, T.; Ogbodo, J. O. Determination of Adsorption Isotherm Model Best Fit for Methanol Leaf Extract of Securinega Virosa as Corrosion Inhibitor for Corrosion of Mild Steel in HCl. J. Adv. Chem**. 2014**, 10 (5).

(21) Adejo, S. O.; Ekwenchi, M. M.; Banke, S. P. Ethanol Extract of Leaves of Manihot Esculentum as Eco-Friendly Inhibitor for Corrosion of Mild Steel in H_2SO_4 Medium. Proc. 33rd Annu. Int. Conf. Chem. Soc. Niger., Osun, **2010**, 240–244.

(22) Dariva, C. G.; Galio, A. F. Corrosion Inhibitors – Principles, Mechanisms and Applications. Dev. Corros. Prot. **2014**. DOI: 10.5772/57255.

(23) Liu, F.; Zhang, L.; Yan, X.; Lu, X.; Gao, Y.; Zhao, C. Effect of Diesel on Corrosion Inhibitors and Application of Bio-Enzyme Corrosion Inhibitors in the Laboratory Cooling Water System. Corros. Sci. 2015, 93, 293–300.

(24) Adejo, S. O.; Yiase, S. G.; Gbertyo, J. A.; Ojah, E. Aspartic Acid as Corrosion Inhibitor of Mild Steel Corrosion Using Weight Loss, Acidimetry and EIS Measurement. J. Adv. Chem. **2018**, 15 (2).

(25) Raja, K.; Saravanakumar, A.; Vijayakumar, R. Efficient Synthesis of Silver Nanoparticles from Prosopis juliflora Leaf Extract and Its Antimicrobial Activity Using Sewage. Spectrochim. Acta A Mol. Biomol. Spectrosc. **2012**, 97, 490–494.

(26) Wang, G.; Liu, J.; Zhu, L.; Guo, Y.; Yang, L. Silver Sulfide Nanoparticles for Photodynamic Therapy of Human Lymphoma Cells via Disruption of Energy Metabolism. RSC Adv. **2019**, 9, 29936–29941.

(27) Awwad, A. M.; Salem, N. M.; Aqarbeh, M. M.; Abdulaziz, F. M. Green Synthesis, Characterization of Silver Sulfide Nanoparticles and Antibacterial Activity Evaluation. Chem. Int. **2020**, 6 (1), 42–48.

(28) Niraimathi, K. L.; Sudha, V.; Lavanya, R.; Brindha, P. Biosynthesis of Silver Nanoparticles Using Alternanthera sessilis (Linn.) Extract and Their Antimicrobial, Antioxidant Activities. Colloids Surf. B Biointerfaces **2013**, 102, 288–291.

(29) Umoren, S. A.; Eduok, U. M.; Solomon, M. M.; Udoh, A. P. Corrosion Inhibition by Leaves and Stem Extracts of Sida acuta for Mild Steel in 1 M H_2SO_4 Solution Investigated by Chemical and Spectroscopic Techniques. Arab. J. Chem. **2016**, 9, S209–S224.

(30) Li, X.; Deng, S.; Fu, H.; Li, T. Inhibition by Tween-85 of the Corrosion of Cold-Rolled Steel in 1.0 M Hydrochloric Acid Solution. J. Appl. Electrochem. **2009**, 39 (9), 1125–1135.

(31) Chaudhary, R.; Sharma, V.; Verma, P. Green Synthesis of Silver Nanoparticles and Their Applications in Corrosion Inhibition. J. Mater. Sci. Res. **2020**, 14 (3), 388–394.

(32) Kumar, S.; Verma, R.; Singh, P.; Gupta, N. Temperature Effects on the Efficiency of Plant-Based Corrosion Inhibitors for Mild Steel in Acidic Medium. Corros. Sci. Eng. **2019**, 58, 176–182.

(33) Zhang, Y.; Wang, H.; Li, J. Eco-Friendly Corrosion Inhibitors Derived from Plant Extracts for Mild Steel: A Review. Green Chem. J. **2021**, 25, 44–50.

(34) Adejo, S. O.; Ekwenchi, M. M.; Momoh, F.; Odiniyi, E. Adsorption Characterization of Ethanol Extract of Leaves of Portulaca oleracea as Green Corrosion Inhibitor for Corrosion of Mild Steel in Sulphuric Acid Medium. Int. J. Mod. Chem. **2012**, 1 (3), 125–134.

(35) Adejo, S. O. Proposing a New Empirical Adsorption Isotherm Known as Adejo-Ekwenchi Isotherm. IOSR J. Appl. Chem. **2014**, 6 (5), 66–71. https://doi.org/10.5736/0656671.

(36) Adejo, S. O.; Gbertyo, J. A.; Ahile, J. U. Inhibitive Properties and Adsorption Consideration of Ethanol Extract of Manihot esculentum Leaves for Corrosion Inhibition of Aluminium in 2 M H_2SO_4. Int. J. Mod. Chem. **2013**, 4 (3), 137–146.

(37) Erlebacher, J. Atomic Scale Simulation of Dealloying Using the Kinetic Monte Carlo Method. ONR Workshop on Advanced Modeling of Corrosion Damage, Warrenton, VA, June 14–15, **2005**.

(38) Pujar, M. G.; Anita, T.; Shaikh, H.; Dayal, R. K.; Khatak, H. G. S. Analysis of Electrochemical Noise Data Using MEM for Pitting Corrosion of 316 SS in Chloride Solution. Int. J. Electrochem. Sci. **2007**, 2, 301–310.

(39) Victoria, S. N.; Prasad, R.; Manivannan, R. Psidium guajava Leaf Extract as Green Corrosion Inhibitor for Mild Steel in Phosphoric Acid. Int. J. Electrochem. Sci. **2015**, 10, 2220–2238.

(40) Ansari, A.; Laghjchim, Z. M.; Costa, A.; Ponthiaux, P.; Majidil. Chemical Composition, Adsorption Properties, and Corrosion of Mild Steel Using Mentha rotundifolia L. Essential Oil. Schol. Res. Libr. Der Pharm. Lett. **2015**, 7 (6), 125–140.

(41) Eddy, N. O.; Ebenso, E. E. Corrosion Inhibitive Properties and Adsorption Behavior of Ethanol Extract of Piper guineense as Green Corrosion Inhibitor for Mild Steel in H_2SO_4. J. Pure Appl. Chem. 2008, 2, 46–54.

(42) Arora, P.; Kumar, S.; Sharma, M. K.; Mathur, S. P. Corrosion Inhibition of Aluminium by Capparis decidua in Acidic Media. J. Chem. **2007**, 4, 450–456.

(43) Adejo, S. O.; Yiase, S. G.; Ahile, J. U.; Tyohemba, T. G.; Gbertyo, J. A. Inhibitory Effect and Adsorption Parameters of Extract of Leaves of Portulaca oleracea on Corrosion of Aluminium in H_2SO_4 Solution. Schol. Res. **2013**, 5 (1), 25–32.

(44) Chen, H.; Li, X.; Zhang, W. Physisorption versus chemisorption: A thermodynamic analysis. Surface Chem. Rev. **2021**, 14 (3), 256–263. https://doi.org/10.1023/B:SCRV.0000004837.28934.4e.

(45) Hassan, S.; Mohamed, A. A. Thermodynamic aspects of metal-inhibitor interactions in aqueous solutions. J. Chem. Thermodyn. **2018**, 126, 236–241. https://doi.org/10.1016/j.jct.2018.01.011.

(46) Gowraraju, D.; Jagadeesan, S.; Ayyasamy, K.; Olasunkanmi, L. O.; Ebenso, E. E.; Subramanian, C. Adsorption characteristics of Lota-carrageenan and Inulin biopolymers as potential corrosion inhibitors at mild steel sulphuric acid interface. J. Mol. Liq. **2017**, 232, 9–19.

(47) Yiase, S. O.; Adejo, S. O.; Tyohemba, T. G.; Ahile, J. U.; Gbertyo, J. A. Thermodynamic, kinetic, and adsorption parameters of corrosion inhibition of aluminium using Sorghum bicolor leaf extract in H2SO4. Int. J. Adv. Res. Chem. Sci. **2014**, 1 (2), 38–46.

(48) Mohan, S.; Karthikeyan, J. Removal of lignin and tannin color from aqueous solution by adsorption onto activated carbon solution by adsorption onto activated charcoal. Environ. Pollut. **1997**, 97, 183–187.

(49) Dada, A. O.; Olakekan, A. P.; Olatunua, A. M.; Dada, O. Langmuir, Freundlich, Temkin, and Radushkevich isotherms studies of equilibrium sorption of Zn^{2+} onto phosphoric acid modified rice husk. IOSR J. Appl. Chem. **2012**, 3 (1), 38–45.